



Published in final edited form as:

NMR Biomed. 2015 October ; 28(10): 1315–1323. doi:10.1002/nbm.3381.

Reproducibility and effect of tissue composition on cerebellar GABA MRS in an elderly population

Zaiyang Long^{a,†}, Jonathan P. Dyke^{b,†}, Ruoyun Ma^{c,d}, Chaorui C. Huang^e, Elan D. Louis^{f,g}, and Ulrike Dydak^{c,d,*}

^aDepartment of Radiology, Mayo Clinic, Rochester, MN, USA

^bDepartment of Radiology, Weill Cornell Medical College, New York, NY, USA

^cSchool of Health Sciences, Purdue University, West Lafayette, IN, USA

^dDepartment of Radiology and Imaging Sciences, Indiana University School of Medicine, Indianapolis, IN, USA

^eBrain and Mind Research Institute, Weill Medical College of Cornell University, New York, NY, USA

^fDepartment of Neurology, Yale School of Medicine, Yale University, New Haven, CT, USA

^gDepartment of Chronic Disease Epidemiology, Yale School of Public Health, Yale University, New Haven, CT, USA

Abstract

Magnetic resonance spectroscopy (MRS) provides a valuable tool to non-invasively detect brain gamma-amino butyric acid (GABA) *in vivo*. GABAergic dysfunction has been observed in the aging cerebellum. Studying cerebellar GABA changes is of considerable interest in understanding certain age-related motor disorders. However, little is known about the reproducibility of GABA MRS in an aged population. Therefore, this study aimed to explore the feasibility and reproducibility of GABA MRS in the aged cerebellum at 3.0 Tesla and to examine the effect of differing tissue composition on GABA measurements. MRI and ¹H MRS exams were performed on 10 healthy elderly volunteers (mean age 75.2 years ± 6.5 years) using a 3.0 Tesla Siemens Tim Trio scanner. Among them, 5 subjects were scanned twice to assess short-term reproducibility. The MEGA-PRESS J-editing sequence was used for GABA detection in two volumes of interest (VOIs) in left and right cerebellar dentate. MRS data processing and quantification were performed with LCModel 6.3-0L using two separate basis sets, generated from density matrix simulations using published values for chemical shifts and J-couplings. Raw metabolite levels from LCModel outputs were corrected for cerebrospinal fluid contamination and relaxation. GABA-edited spectra yielded robust and stable GABA measurements with averaged intra-individual coefficients of variation for corrected GABA+ between 4.0 ± 2.8 % to 13.4 ± 6.3 % and inter-individual coefficients of variation between 12.6 % and 24.2 %. In addition, there was a significant correlation between GABA+ obtained with the two LCModel basis sets. Overall our

*Correspondence to: U. Dydak, School of Health Sciences, Purdue University, West Lafayette, IN, 47907, USA. udydak@purdue.edu.

†These authors contributed equally to the work.

results demonstrated the feasibility and reproducibility of cerebellar GABA-edited MRS at 3.0 Tesla in an elderly population. This information might be helpful for studies that use this technique to study GABA changes in normal or diseased aging brain, e.g., for power calculations and interpretation of longitudinal observations.

Keywords

magnetic resonance spectroscopy (MRS); gamma-amino butyric acid (GABA); aging brain; reproducibility; partial volume correction

INTRODUCTION

The precise balance between excitatory and inhibitory neurotransmitter systems is critical for maintaining the function of the central nervous system. Inhibition is mediated by gamma-amino butyric acid (GABA) through actions on both ionotropic and metabotropic receptors. In the developing nervous system, GABA plays a key role in modulating neural progenitor proliferation, cell migration, and circuit formation (1). In the normal aging brain, decrease in GABAergic parameters, such as reduced GABA current amplitude and loss in GABA-immunopositive neurons, is known to affect brain functions such as visual acuity and orientation sensitivity (2–5). Moreover, disturbances of the GABA neurotransmitter system have been implicated in many neurological and psychiatric diseases, including epilepsy (6), mood and anxiety disorders (7,8), sleep disorders (9), schizophrenia (10), autism (11) and essential tremor (12). Understanding *in vivo* GABA changes would provide important insights into the mechanism of age-related brain function deficits and the role of GABA in various disease models, as well as aid in potential treatment evaluations.

Currently, magnetic resonance spectroscopy (MRS) provides a valuable tool to non-invasively detect brain metabolites *in vivo*. While it has proven to be difficult to reliably measure *in vivo* GABA due to its low concentration and spectral overlap with other more abundant metabolites, several methods have been adapted to successfully measure GABA, among which the most frequently used is the MEGA-PRESS sequence (13–15). Indeed, MRS studies have shown GABA perturbation in the above mentioned neurological and psychiatric diseases (16–21). Several groups also reported age-associated decreases in brain GABA levels in humans and rodents (22,23). In addition, reduced cortical GABA was demonstrated in elderly patients with mild cognitive impairment (24). A better understanding of the reproducibility of the technique in an aged population would aid in associating these changes to motor, sensory and cognitive deficits.

Several studies reported within-session, short-term and long-term reproducibility of brain GABA MRS measurements, with coefficients of variation (CVs) differing across studies, but generally less than 20%, depending on brain regions, acquisition parameters and spectral fitting tools (25–32). However, all of these studies recruited a young subject population (mean age of these eight studies: 29 years). The aging brain is known to suffer from substantial structural and neurochemical changes compared to the young brain (33). Losses in brain tissue volumes due to age-related atrophy also differ substantially between white matter (WM), gray matter (GM) and cerebrospinal fluid (CSF) (34). Therefore, the results

obtained from the young population may not be generalized to an elderly population. Assessment of the reproducibility of GABA MRS measurements and effects of tissue composition in an elderly population might provide new and relevant information for studies that explore GABA changes in normal and diseased aging brain regions. For example, one region of interest is the cerebellum, which does not only show age-related volumetric change, but is also involved in age-related motor deficits, learning function and processing speed decline (33,35–37). GABAergic dysfunction has been observed in the aging cerebellum and seems to be of great interest in age-related motor and cognitive deficits (38–40). One of the potential targets is to study essential tremor, the most common cause of tremor in humans. Increased ^{11}C -flumazenil binding at GABAergic receptor sites was reported by a positron emission tomography study (38), suggesting the potential involvement of GABA activity in essential tremor.

The aims of the current analyses were to 1) explore the feasibility and reproducibility of GABA-edited spectroscopy in the aged cerebellum at 3.0 Tesla, 2) examine the effect of tissue composition on GABA measurements.

MATERIALS AND METHODS

Subjects

A group of 10 healthy elderly volunteers (three males, seven females; age: mean \pm standard deviation [SD], 75.2 ± 6.5 years, ranging from 65 to 86 years) were recruited as part of a longitudinal study of brain GABA in patients with essential tremor and age-matched healthy elderly volunteers. All healthy elderly volunteers underwent a structured clinical interview to rule out any neurological or psychiatric diseases as well as a detailed videotaped neurological examination that was reviewed by a senior movement disorder neurologist (EDL) to rule out the presence of essential tremor, Parkinson's disease or other disorders of involuntary movement. None of the volunteers was taking medication that could increase brain GABA concentration (e.g., clonazepam, primidone) or had a history of heavy exposure to ethanol, as previously defined (41). To assess short-term intra-individual reproducibility, 5 healthy volunteers were scanned twice with varied time intervals ranging from 2 to 28 days (Mean \pm SD: 10.8 ± 8.9 days). The study protocol was reviewed and approved by the Human Subjects Institutional Review Board at Columbia University, Yale University, Purdue University and at Weill Cornell Medical College. Written informed consent was obtained from each subject prior to participation in the study.

In vivo MRI/MRS measurements

MRI and ^1H MRS exams were performed on a 3.0 Tesla Siemens Tim Trio scanner (Siemens Healthcare, Erlangen, Germany), equipped with a 32-channel head coil. Fast T_2 -weighted images were acquired in all three orientations to ensure exact localization of the MRS volumes of interest (VOIs). Short-TE ^1H spectra (PRESS localization; TR/TE = 1500/30 ms; CHESS water suppression) were acquired in four volumes of interest (VOIs): left and right cerebellar cortex (both $15\text{ mm} \times 15\text{ mm} \times 25\text{ mm}$, 128 averages), and left and right cerebellar dentate nucleus (both $25\text{ mm} \times 25\text{ mm} \times 25\text{ mm}$, 128 averages) (Figure 1). For all of the VOIs, a reference spectrum was acquired without water suppression. These

reference spectra were then used for phase and frequency correction of the corresponding water-suppressed spectra. FASTESTMAP shimming (IPR#577; Siemens Healthcare) was performed before each voxel measurement to achieve water line widths of < 20 Hz (42). The MEGA-PRESS J-editing sequence was used for GABA detection (TR/TE = 1500/68 ms) (13,14) in two of the four VOIs described above. MEGA-PRESS spectra were only acquired in the right and left dentate nucleus, given the fact that this is the level at which the Purkinje cells release their GABA into the synaptic cleft (43). 196 averages were acquired with the spectrally selective editing pulse centered at 1.9 ppm (edit-on) and 196 averages with the pulse centered at 7.5 ppm (edit-off) in an interleaved fashion. The resulting difference spectrum contains a GABA peak at 3.0 ppm, which also includes contributions from co-edited macromolecules and homocarnosine, a dipeptide consisting of GABA and histidine. Therefore, the signal will be referred to as GABA+. In order to determine voxel tissue composition, high-resolution MPRAGE images were acquired (TR/TE/TI = 2300/2.91/900 ms, flip angle = 9°, bandwidth: 240 Hz/pixel, voxel size: 1.0 mm × 1.0 mm × 1.2 mm, GRAPPA = 2). Every effort was made to ensure the subjects were as comfortable as possible in the scanner. The dentate nucleus was clearly identified on the T₂-weighted images on both axial and coronal planes. The GABA voxel was placed on the axial plane such that the entire dentate nucleus was included while minimizing contributions from vascular and CSF compartments. The voxel was then confirmed to be completely within the cerebellum on the coronal plane. The voxel placed in the cerebellar cortex was placed in the posterior cortex of the axial plane and the superior cortex on the coronal plane. The voxel was angled to follow the edge of the cerebellar cortex in both axial and coronal planes. Placement was then confirmed to be completely contained within the cerebellum on the sagittal plane. Using this prescription allowed for reproducible placement of voxels across subjects and in repeat scans.

Data processing and analysis

MRS data processing and quantification were performed with LCModel 6.3-0L (44), fitting each spectrum as a weighted linear combination of basis spectra from individual metabolites. For the short-TE spectra, a basis set of *in vitro* spectra from individual metabolite solutions was used. For the MEGA-PRESS spectra, basis sets were generated from density matrix simulations of the sequence using two sets of published values for chemical shifts and J-couplings from Govindaraju et al. and Kaiser et al. (45,46), with an exact treatment of metabolite evolution during the two frequency-selective MEGA inversion pulses. These two sets of chemical shift and J-coupling values (Table 1), one from an early publication reporting multiple metabolites and one from a later publication for refining GABA values, have been used extensively in GABA spectroscopy studies to date. Therefore, we chose to analyze our MEGA-PRESS spectra with two separate basis sets that employed both sets of values, and to further test their relationship. The two basis sets are denoted as “Govindaraju basis set” and “Kaiser basis set”, or abbreviated as G basis set and K basis set, respectively. Difference basis spectra were obtained by subtracting the simulated metabolite response to selective inversion at 7.5 ppm from that at 1.9 ppm.

Full width half maximum (FWHM) and signal to noise ratio (S/N) were checked to ensure consistent spectral quality. Two sets of short-TE spectra from the cerebellar cortex VOIs

were excluded from further analysis due to insufficient water suppression. LCModel fitting %SD values for our metabolites of interest - creatine (Cr), N-acetyl aspartate (NAA) and glutamate (Glu) - were lower than 10 %, and GABA+ lower than 20 %.

In order to compare results with previous published reports, the ratios of GABA+ over Cr and NAA were also calculated. While raw GABA+/NAA values were directly given by LCModel outputs, raw GABA+ values were derived from raw water-scaled GABA+ output values, multiplied by a water scaling factor. Cr levels were obtained from spectra with the MEGA-PRESS editing pulse centered at 7.5 ppm, in order to calculate the ratios of GABA +/Cr. To determine the tissue composition of the voxels, MPRAGE images were segmented into GM, WM and CSF using an in-house MATLAB 2013a tool (MathWorks Inc., Natick, MA, USA) incorporated with statistical parametric mapping (SPM8, Wellcome Department of Imaging Neuroscience, London, United Kingdom). One segmentation example of a dentate nucleus voxel is shown in Figure 2. Metabolite levels corrected for CSF and relaxation were obtained using the following equation (47,48),

$$M_{cor} = (M_{raw}) \times \frac{43300 \times f_{GM} + 35880 \times f_{WM} + 55556 \times f_{CSF}}{35880} \times \frac{1}{1 - f_{CSF}} \times VIS_w \times \frac{\exp(-\frac{TE}{T2_{water}})}{\exp(-\frac{TE}{T2_m})}$$

where M_{cor} is the corrected value, M_{raw} is the uncorrected value, VIS_w is a correcting factor for MR water visibility (0.65), $T2_m$ is the T2 relaxation time of the metabolite, and f_{GM} , f_{WM} and f_{CSF} are the fraction of GM, WM and CSF within the voxel, respectively. The term $(43300 \times f_{GM} + 35880 \times f_{WM} + 55556 \times f_{CSF})/35880$ is included to adjust for voxel water concentration, where the LCModel default water concentration is 35880. CSF contamination is corrected for by the term $1/(1-f_{CSF})$. LCModel estimates T1 relaxation

correction through $f = \frac{1}{1 - \exp(-TR/T1)}$ when water scaling is used. Therefore, no additional correction for T1 relaxation was performed. T2 of GABA, Cr, NAA, Glu and water were chosen to be 88, 154, 259, 181 and 95 ms, respectively (49–51). For GABA, raw output from the difference spectrum should be multiplied by FCALIB factor, which can be obtained from the .PRINT file from the edit-off spectrum analysis to estimate water scaled concentration. Corrected metabolite ratios were calculated from corrected GABA+ divided by corrected Cr and corrected NAA, respectively. Both raw and corrected levels are reported.

Statistics

Results from a total of 30 GABA-edited spectra from the cerebellar dentate, 30 short-TE spectra from the cerebellar dentate and 28 from the cerebellar cortex were analyzed. Statistical analyses were performed using SPSS 21.0 (IBM Corp., Armonk, NY, USA). All metabolites of interest were found to be normally distributed, as assessed by the Shapiro-Wilk test ($p > 0.05$). Descriptive values are reported (mean, SD). CVs for each of the 5 individuals who underwent two scans were calculated and averaged as an estimate of intra-individual reproducibility, while CVs for all subjects were calculated as an estimate of inter-individual reproducibility for each metabolite of interest. Metabolite levels were compared between left and right corresponding VOIs using Student's t-tests. Pearson's correlation was

used to estimate the relationship between combined left and right corrected GABA+, versus raw GABA+, GABA+/Cr and GABA+/NAA measurements. The correlations between combined left and right NAA and Glu in cerebellar dentate and cortex were also determined, respectively, in order to compare with one previous publication, which found a significant correlation in young subjects (52). In order to compare the performance of the two basis sets, pairwise Wilcoxon signed rank tests were used to test the mean values of all raw and corrected GABA+ measurements, and the corresponding inter- and intra-individual CVs between using the two basis sets. Bonferroni correction was employed to correct for multiple comparisons.

RESULTS

Figure 1 shows representative VOI placements for right cerebellar cortex and dentate, as well as pairs of right cerebellar GABA-edited difference spectra from 5 subjects. GABA+ measurements (GABA+, GABA+/Cr and GABA+/NAA) including raw and corrected values using two sets of LCModel analysis are reported in Table 2. Intra-individual CVs for the repeated GABA+ measurements (raw and corrected GABA+, GABA+/Cr and GABA+/NAA) range from $4.0 \pm 2.8\%$ to $13.9 \pm 6.9\%$, whereas inter-individual CVs range from 12.6% to 27.0% . Overall correction for CSF contamination and relaxation did not significantly improve the CVs. No difference was observed between left and right cerebellar dentate GABA+ levels. Corrected Cr, NAA and Glu levels obtained from the short-TE spectra in all four VOIs are shown in Table 3. Intra-individual CVs for these corrected metabolites were lower than $5.5 \pm 0.5\%$, while inter-individual CVs were lower than 15.4% . NAA levels were significantly higher in the left than in the right cerebellar cortex ($p < 0.001$). In addition, there was a significant correlation between NAA and Glu in the cerebellar cortex ($R = 0.699$, $p < 0.01$), but not in the dentate.

Figure 3 shows the individual corrected GABA+ levels in left and right cerebellar dentate from all subjects using two LCModel basis sets, with 5 of them scanned twice for assessing short-term reproducibility. Using the Kaiser basis set, corrected GABA+ significantly correlated with raw GABA+, GABA+/Cr and GABA+/NAA ($R = 0.985$, 0.869 and 0.857 , respectively, all p values < 0.001) (Fig. 4). Using Govindaraju basis set, corrected GABA+ levels also significantly correlated with raw GABA+, GABA+/Cr and GABA+/NAA ($R = 0.965$, 0.729 and 0.737 , respectively, all p values < 0.001). Corrected GABA+ using the Kaiser basis set and the Govindaraju basis set were significantly different ($p < 0.01$). However, they did show a significant correlation ($R = 0.858$, $p < 0.001$). For all raw and corrected measurements, using the Kaiser basis set yielded smaller GABA values and higher inter-individual CVs than using the Govindaraju basis set, as shown by pairwise Wilcoxon signed ranks tests (both $p < 0.01$). No significant difference was seen in intra-individual CVs between the two basis sets. Table 4 shows percentages of tissue compositions of all 4 VOIs. No significant difference was observed between left and right cortical or dentate voxel composition.

DISCUSSION

Our results demonstrate the feasibility of cerebellar GABA-edited spectroscopy at 3.0 Tesla in an elderly population with a mean age of 75.2 years. In general, using the Kaiser basis set yielded smaller GABA+ values than using the Govindaraju basis set, which should be due to the fact that Kaiser et al. considered realistic experimental issues such as volume selection, radiofrequency pulse shapes, editing efficiency, etc., leading to significant signal loss compared to ideal conditions. No significant difference in intra-individual CVs was observed between using the two basis sets. However, inter-individual CVs were higher using the Kaiser basis set. This could be due to mean GABA+ values being lower using the Kaiser basis set, resulting in a smaller denominator for calculating inter-individual CVs and thus higher CVs (corrected GABA+ (mean \pm SD): 1.10 ± 0.23 for Kaiser basis set while 1.46 ± 0.21 for Govindaraju basis set).

Two recent studies have shown GABA-edited spectra in the cerebellar vermis and left cerebellum in a younger healthy population (mean age: 24.6 and 43.5 years, GABA+/Cr 0.23 ± 0.06 and 0.21 ± 0.09 , respectively) (52,53). Our GABA+/Cr levels were found to be in similar ranges—in the left cerebellum, corrected GABA+/Cr value was 0.22 ± 0.05 using the Kaiser basis set and 0.30 ± 0.04 using the Govindaraju basis set; while averaged left and right cerebellar GABA+/Cr was 0.23 ± 0.05 using the Kaiser basis set and 0.31 ± 0.05 using the Govindaraju basis set. In the literature no change or increased Cr were found (54,55), while no change or decreased GABA were reported in older subjects (22–24,56). GABA +/Cr values calculated with the Kaiser basis set were more similar with the reported GABA/Cr values in a young population, whereas the GABA+/Cr levels calculated with the Govindaraju basis set were slightly higher than that in younger populations. If using literature values as gold standard, this finding may reflect the fact that Kaiser et al. actually refined GABA chemical shifts and J-coupling values compared to Govindaraju et al. Yet, it is unknown what chemical shifts and/or coupling constants were used for the reported values. Therefore, direct comparison may be problematic. The current study suggests that one needs to be aware of the different outcomes when using these basis sets. It is important for the authors to report how their basis sets were simulated and comparisons with literature values must take this difference into account. It is worth mentioning that there was still a significant correlation between GABA levels obtained from both basis sets.

Corrected NAA levels in our study were lower than corrected Cr levels in all 4 VOIs. Guerrini et al. (57) reported corrected NAA/Cr = 0.79 ± 0.17 in a VOI that included the superior cerebellar vermis from 29 healthy subjects (age 37 ± 11 years). Our mean corrected NAA/Cr was 0.73 ± 0.09 in the cerebellar cortex, a similar VOI to their VOI. In addition, mean raw NAA/Cr can be derived as 1.08 in the cerebellum of elderly subjects from Zahr et al. (54), while our mean raw NAA/Cr was 1.00 ± 0.11 in a similar VOI in the dentate nucleus. The currently reported intra- and inter-individual CVs of cerebellar NAA and Cr are also in close agreement with previous reports (58,59). It is worthwhile noting here that different investigators, and hence different studies, may use different acquisition parameters, voxel sizes/placements and spectra quantification tools. Thus, absolute values are difficult to directly compare with each other; even metabolite ratios may differ slightly without real physiological cause.

The asymmetry between left and right cerebellar cortical NAA levels is in line with two previous reports on higher NAA in the left prefrontal cortex and left thalamus from healthy subjects (60,61). In fact, a greater neuronal density was observed in the left than in the right hemisphere in the literature (62,63). The current correlation between NAA and Glu in the cerebellar cortex, but not in the dentate, is in general agreement with Waddell et al. (52), because their cerebellar vermis VOI contained more cortical regions.

The reproducibility studies on GABA MRS in younger adult populations reported intra-individual CVs for GABA+ to be between 3.5 % and 20.4 %, whereas inter-individual CVs were between 9.1 % and 38 %, depending on different brain regions, acquisition and analysis techniques (25–32). It is important to mention that three of these reports appear not to have corrected for CSF contamination, however, they did not necessarily have higher CVs. Despite being conducted in an elderly study population, our corrected GABA+ showed similar reproducibility results (mean intra-individual CVs between 4.0 % and 13.4 % and inter-individual CVs between 12.6 % and 24.2 %). Though supposed to be corrected for inter-individual differences in neuronal density and atrophy, CSF- and relaxation-corrected GABA+ levels still significantly correlated with raw GABA+, GABA+/Cr and GABA+/NAA in the dentate nucleus calculated with both Kaiser and Govindaraju basis sets in this elderly population. Correction for CSF and relaxation did not improve the reproducibility results, which may be due to the very small CSF volume in the voxel (< 5.3 % for both dentate VOIs) and the larger difference in measured GABA+ values among these differently aged subjects (between 65 and 86 years). Nevertheless, correction would still be critical and considered as an important factor to control in studying older subjects, who may have volume loss and atrophy in the region of interest.

One major limitation of the current MEGA-PRESS sequence is macromolecular contamination of the GABA signal at 3.0 ppm. This could be corrected by placing the editing pulses at 1.9 and 1.5 ppm in order to symmetrically suppress macromolecules at 3.0 ppm (64), but often this results in substantial suppression of GABA due to insufficient selectivity of the editing pulse at 3.0 Tesla. This technique is also impractical in an aged population, which likely has decreased GABA levels. Alternatively, the contamination problem could be addressed by using other sequences for acquisition or by explicitly modeling the macromolecules in the LCModel basis set in post-processing procedures (65,66). Nevertheless, the current study chose to use the original MEGA-PRESS sequence and direct LCModel analysis to evaluate GABA reproducibility, because of the availability and practicability of this approach, especially in a clinical study. Our results need to be interpreted as showing the short-time reproducibility of measuring the sum of GABA, homocarnosine and co-edited macromolecules in the cerebellum of an elderly population. In addition, our basis sets were created assuming ideal pulses, therefore, they actually correspond to the center point in the voxel. Consequently the resulting quantification would slightly overestimate true metabolite levels due to spatial variation in excitation, refocusing, and chemical shift misregistration.

CONCLUSIONS

In summary, our results demonstrated the feasibility of cerebellar GABA-edited MRS at 3.0 Tesla in an elderly population. All GABA measurements yielded reproducible estimates using the MEGA-PRESS sequence, with the approach using the Kaiser basis set yielding quantification results of GABA+/Cr that were most consistent with literature reports. With a small CSF percentage in the dentate VOIs and a large range in age amongst the elderly subjects (~20 years), correction for CSF contamination and relaxation did not improve the reproducibility results. Corrected GABA+ levels significantly correlated with uncorrected GABA+ measurements. These results might be helpful for any study that uses this technique to examine GABA changes in normal or diseased aging brain, e.g., for power calculation and interpretation of longitudinal observations.

ACKNOWLEDGEMENTS

This work was supported by NINDS R01 NS085136 and NIEHS R01 ES020529 from the National Institutes of Health. The authors would like to thank Dr. Nora Hernandez for her assistance in subject recruitment. The authors also thank James Murdoch for generating LCModel basis sets and Shalmali Dharmadhikari for assistance in initial experiment testing.

Abbreviations used

CSF	cerebrospinal fluid
CV	coefficient of variation
FWHM	full width half maximum
GABA	gamma-amino butyric acid
Glu	glutamate
GM	gray matter
NAA	N-acetyl aspartate
Cr	creatine
SD	standard deviation
S/N	signal to noise ratio
VOI	volume of interest
WM	white matter

REFERENCES

1. Lehmann K, Steinecke A, Bolz J. GABA through the Ages: Regulation of Cortical Function and Plasticity by Inhibitory Interneurons. *Neural Plast.* 2012
2. Hua T, Kao C, Sun Q, Li X, Zhou Y. Decreased proportion of GABA neurons accompanies age-related degradation of neuronal function in cat striate cortex. *Brain Res Bull.* 2008; 75(1):119–125. [PubMed: 18158105]
3. Leventhal AG, Wang Y, Pu M, Zhou Y, Ma Y. GABA and its agonists improved visual cortical function in senescent monkeys. *Science.* 2003; 300(5620):812–815. [PubMed: 12730605]

4. Ferrer-Blasco T, Gonzalez-Mejome JM, Montes-Mico R. Age-related changes in the human visual system and prevalence of refractive conditions in patients attending an eye clinic. *J Cataract Refract Surg.* 2008; 34(3):424–432. [PubMed: 18299067]
5. Spear PD. Neural bases of visual deficits during aging. *Vision Res.* 1993; 33(18):2589–2609. [PubMed: 8296455]
6. Treiman DM. GABAergic mechanisms in epilepsy. *Epilepsia.* 2001; 42(Suppl 3):8–12. [PubMed: 11520315]
7. Brambilla P, Perez J, Barale F, Schettini G, Soares JC. GABAergic dysfunction in mood disorders. *Mol Psychiatry.* 2003; 8(8):721–737. 715. [PubMed: 12888801]
8. Malizia AL. What do brain imaging studies tell us about anxiety disorders? *Journal of Psychopharmacology.* 1999; 13(4):372–378. [PubMed: 10667613]
9. Gottesmann C. GABA mechanisms and sleep. *Neuroscience.* 2002; 111(2):231–239. [PubMed: 11983310]
10. Lewis DA. GABAergic local circuit neurons and prefrontal cortical dysfunction in schizophrenia. *Brain Res Brain Res Rev.* 2000; 31(2–3):270–276. [PubMed: 10719153]
11. Fatemi SH, Reutiman TJ, Folsom TD, Thuras PD. GABA(A) receptor downregulation in brains of subjects with autism. *J Autism Dev Disord.* 2009; 39(2):223–230. [PubMed: 18821008]
12. Louis ED. A new twist for stopping the shakes? Revisiting GABAergic therapy for essential tremor. *Arch Neurol.* 1999; 56(7):807–808. [PubMed: 10404981]
13. Mescher M, Merkle H, Kirsch J, Garwood M, Gruetter R. Simultaneous in vivo spectral editing and water suppression. *NMR Biomed.* 1998; 11(6):266–272. [PubMed: 9802468]
14. Edden RA, Barker PB. Spatial effects in the detection of gamma-aminobutyric acid: improved sensitivity at high fields using inner volume saturation. *Magn Reson Med.* 2007; 58(6):1276–1282. [PubMed: 17969062]
15. Puts NA, Edden RA. In vivo magnetic resonance spectroscopy of GABA: a methodological review. *Prog Nucl Magn Reson Spectrosc.* 2012; 60:29–41. [PubMed: 22293397]
16. Chowdhury FA, O’Gorman RL, Nashef L, Elwes RD, Edden RA, Murdoch JB, Barker GJ, Richardson MP. Investigation of glutamine and GABA levels in patients with idiopathic generalized epilepsy using MEGAPRESS. *J Magn Reson Imaging.* 2015; 41(3):694–699. [PubMed: 24585443]
17. Winkelman JW, Buxton OM, Jensen JE, Benson KL, O’Connor SP, Wang W, Renshaw PF. Reduced brain GABA in primary insomnia: preliminary data from 4T proton magnetic resonance spectroscopy (1H-MRS). *Sleep.* 2008; 31(11):1499–1506. [PubMed: 19014069]
18. Yoon JH, Maddock RJ, Rokem A, Silver MA, Minzenberg MJ, Ragland JD, Carter CS. GABA concentration is reduced in visual cortex in schizophrenia and correlates with orientation-specific surround suppression. *J Neurosci.* 2010; 30(10):3777–3781. [PubMed: 20220012]
19. Rojas DC, Singel D, Steinmetz S, Hepburn S, Brown MS. Decreased left perisylvian GABA concentration in children with autism and unaffected siblings. *Neuroimage.* 2014; 86:28–34. [PubMed: 23370056]
20. van der Hel WS, van Eijnsden P, Bos IW, de Graaf RA, Behar KL, van Nieuwenhuizen O, de Graan PN, Braun KP. In vivo MRS and histochemistry of status epilepticus-induced hippocampal pathology in a juvenile model of temporal lobe epilepsy. *NMR Biomed.* 2013; 26(2):132–140. [PubMed: 22806932]
21. Levy LM, Degnan AJ. GABA-based evaluation of neurologic conditions: MR spectroscopy. *AJNR Am J Neuroradiol.* 2013; 34(2):259–265. [PubMed: 22268095]
22. Gao F, Edden RA, Li M, Puts NA, Wang G, Liu C, Zhao B, Wang H, Bai X, Zhao C, Wang X, Barker PB. Edited magnetic resonance spectroscopy detects an age-related decline in brain GABA levels. *Neuroimage.* 2013; 78:75–82. [PubMed: 23587685]
23. Duarte JM, Do KQ, Gruetter R. Longitudinal neurochemical modifications in the aging mouse brain measured in vivo by 1H magnetic resonance spectroscopy. *Neurobiol Aging.* 2014; 35(7):1660–1668. [PubMed: 24560998]
24. Riese F, Gietl A, Zolch N, Henning A, O’Gorman R, Kalin AM, Leh SE, Buck A, Warnock G, Edden RA, Luechinger R, Hock C, Kollias S, Michels L. Posterior cingulate gamma-aminobutyric acid and glutamate/glutamine are reduced in amnesic mild cognitive impairment and are unrelated

- to amyloid deposition and apolipoprotein E genotype. *Neurobiol Aging*. 2015; 36(1):53–59. [PubMed: 25169676]
25. Evans CJ, McGonigle DJ, Edden RA. Diurnal stability of gamma-aminobutyric acid concentration in visual and sensorimotor cortex. *J Magn Reson Imaging*. 2010; 31(1):204–209. [PubMed: 20027589]
 26. Stephenson MC, Gunner F, Napolitano A, Greenhaff PL, Macdonald IA, Saeed N, Vennart W, Francis ST, Morris PG. Applications of multi-nuclear magnetic resonance spectroscopy at 7T. *World J Radiol*. 2011; 3(4):105–113. [PubMed: 21532871]
 27. Wijtenburg SA, Rowland LM, Edden RA, Barker PB. Reproducibility of brain spectroscopy at 7T using conventional localization and spectral editing techniques. *J Magn Reson Imaging*. 2013; 38(2):460–467. [PubMed: 23292856]
 28. Bogner W, Gruber S, Doelken M, Stadlbauer A, Ganslandt O, Boettcher U, Trattnig S, Doerfler A, Stefan H, Hammen T. In vivo quantification of intracerebral GABA by single-voxel (1)H-MRS-How reproducible are the results? *Eur J Radiol*. 2010; 73(3):526–531. [PubMed: 19201120]
 29. O'Gorman RL, Michels L, Edden RA, Murdoch JB, Martin E. In vivo detection of GABA and glutamate with MEGA-PRESS: reproducibility and gender effects. *J Magn Reson Imaging*. 2011; 33(5):1262–1267. [PubMed: 21509888]
 30. Near J, Andersson J, Maron E, Mекle R, Gruetter R, Cowen P, Jezzard P. Unedited in vivo detection and quantification of gamma-aminobutyric acid in the occipital cortex using short-TE MRS at 3 T. *NMR Biomed*. 2013; 26(11):1353–1362. [PubMed: 23696182]
 31. Near J, Ho YC, Sandberg K, Kumaragamage C, Blicher JU. Long-term reproducibility of GABA magnetic resonance spectroscopy. *Neuroimage*. 2014; 99:191–196. [PubMed: 24875142]
 32. Geramita M, van der Veen JW, Barnett AS, Savostyanova AA, Shen J, Weinberger DR, Marengo S. Reproducibility of prefrontal gamma-aminobutyric acid measurements with J-edited spectroscopy. *NMR Biomed*. 2011; 24(9):1089–1098. [PubMed: 21290458]
 33. Raz N, Rodrigue KM. Differential aging of the brain: patterns, cognitive correlates and modifiers. *Neurosci Biobehav Rev*. 2006; 30(6):730–748. [PubMed: 16919333]
 34. Ge Y, Grossman RI, Babb JS, Rabin ML, Mannon LJ, Kolson DL. Age-related total gray matter and white matter changes in normal adult brain. Part I: volumetric MR imaging analysis. *AJNR Am J Neuroradiol*. 2002; 23(8):1327–1333. [PubMed: 12223373]
 35. Holtzer R, Epstein N, Mahoney JR, Izzetoglu M, Blumen HM. Neuroimaging of Mobility in Aging: A Targeted Review. *J Gerontol A Biol Sci Med Sci*. 2014; 69(11):1375–1388. [PubMed: 24739495]
 36. Woodruff-Pak DS, Goldenberg G, Downey-Lamb MM, Boyko OB, Lemieux SK. Cerebellar volume in humans related to magnitude of classical conditioning. *Neuroreport*. 2000; 11(3):609–615. [PubMed: 10718323]
 37. Louis ED. Essential tremors: a family of neurodegenerative disorders? *Arch Neurol*. 2009; 66(10):1202–1208. [PubMed: 19822775]
 38. Boecker H, Weindl A, Brooks DJ, Ceballos-Baumann AO, Liedtke C, Miederer M, Sprenger T, Wagner KJ, Miederer I. GABAergic dysfunction in essential tremor: an 11C-flumazenil PET study. *J Nucl Med*. 2010; 51(7):1030–1035. [PubMed: 20554735]
 39. Araki T, Kato H, Fujiwara T, Itoyama Y. Regional age-related alterations in cholinergic and GABAergic receptors in the rat brain. *Mech Ageing Dev*. 1996; 88(1–2):49–60. [PubMed: 8803921]
 40. Bickford P. Motor learning deficits in aged rats are correlated with loss of cerebellar noradrenergic function. *Brain Res*. 1993; 620(1):133–138. [PubMed: 8402185]
 41. Harasymiw JW, Bean P. Identification of heavy drinkers by using the early detection of alcohol consumption score. *Alcohol Clin Exp Res*. 2001; 25(2):228–235. [PubMed: 11236837]
 42. Gruetter R, Tkac I. Field mapping without reference scan using asymmetric echo-planar techniques. *Magnet Reson Med*. 2000; 43(2):319–323.
 43. Gambarana C, Loria CJ, Siegel RE. GABAA receptor messenger RNA expression in the deep cerebellar nuclei of Purkinje cell degeneration mutants is maintained following the loss of innervating Purkinje neurons. *Neuroscience*. 1993; 52(1):63–71. [PubMed: 8381926]

44. Provencher SW. Estimation of metabolite concentrations from localized in vivo proton NMR spectra. *Magn Reson Med*. 1993; 30(6):672–679. [PubMed: 8139448]
45. Govindaraju V, Young K, Maudsley AA. Proton NMR chemical shifts and coupling constants for brain metabolites. *NMR Biomed*. 2000; 13(3):129–153. [PubMed: 10861994]
46. Kaiser LG, Young K, Meyerhoff DJ, Mueller SG, Matson GB. A detailed analysis of localized J-difference GABA editing: theoretical and experimental study at 4 T. *NMR Biomed*. 2008; 21(1):22–32. [PubMed: 17377933]
47. Mullins PG, McGonigle DJ, O'Gorman RL, Puts NAJ, Vidyasagar R, Evans CJ, Edden RAE, GABA CSM. Current practice in the use of MEGA-PRESS spectroscopy for the detection of GABA. *Neuroimage*. 2014; 86:43–52. [PubMed: 23246994]
48. Anglin RE, Rosebush PI, Noseworthy MD, Tarnopolsky M, Weber AM, Soreni N, Mazurek MF. Metabolite measurements in the caudate nucleus, anterior cingulate cortex and hippocampus among patients with mitochondrial disorders: a case-control study using proton magnetic resonance spectroscopy. *CMAJ Open*. 2013; 1(1):E48–E55.
49. Edden RA, Intrapiromkul J, Zhu H, Cheng Y, Barker PB. Measuring T2 in vivo with J-difference editing: application to GABA at 3 Tesla. *J Magn Reson Imaging*. 2012; 35(1):229–234. [PubMed: 22045601]
50. Kirov II, Fleysher L, Fleysher R, Patil V, Liu S, Gonen O. Age dependence of regional proton metabolites T2 relaxation times in the human brain at 3 T. *Magn Reson Med*. 2008; 60(4):790–795. [PubMed: 18816831]
51. Ganji SK, Banerjee A, Patel AM, Zhao YD, Dimitrov IE, Browning JD, Brown ES, Maher EA, Choi C. T2 measurement of J-coupled metabolites in the human brain at 3T. *NMR Biomed*. 2012; 25(4):523–529. [PubMed: 21845738]
52. Waddell KW, Zanjani P, Pradhan S, Xu L, Welch EB, Joers JM, Martin PR, Avison MJ, Gore JC. Anterior cingulate and cerebellar GABA and Glu correlations measured by (1)H J-difference spectroscopy. *Magn Reson Imaging*. 2011; 29(1):19–24. [PubMed: 20884148]
53. Winkelman JW, Schoerling L, Platt S, Jensen JE. Restless legs syndrome and central nervous system gamma-aminobutyric acid: preliminary associations with periodic limb movements in sleep and restless leg syndrome symptom severity. *Sleep Med*. 2014; 15(10):1225–1230. [PubMed: 25129262]
54. Zahr NM, Mayer D, Pfefferbaum A, Sullivan EV. Low striatal glutamate levels underlie cognitive decline in the elderly: evidence from in vivo molecular spectroscopy. *Cereb Cortex*. 2008; 18(10):2241–2250. [PubMed: 18234683]
55. Zahr NM, Mayer D, Rohlfing T, Chanraud S, Gu M, Sullivan EV, Pfefferbaum A. In vivo glutamate measured with magnetic resonance spectroscopy: behavioral correlates in aging. *Neurobiol Aging*. 2013; 34(4):1265–1276. [PubMed: 23116877]
56. Aufhaus E, Weber-Fahr W, Sack M, Tunc-Skarka N, Oberthuer G, Hoerst M, Meyer-Lindenberg A, Boettcher U, Ende G. Absence of changes in GABA concentrations with age and gender in the human anterior cingulate cortex: a MEGA-PRESS study with symmetric editing pulse frequencies for macromolecule suppression. *Magnetic resonance in medicine : official journal of the Society of Magnetic Resonance in Medicine / Society of Magnetic Resonance in Medicine*. 2013; 69(2):317–320.
57. Guerrini L, Belli G, Mazzoni L, Foresti S, Ginestroni A, Della Nave R, Diciotti S, Mascalchi M. Impact of cerebrospinal fluid contamination on brain metabolites evaluation with 1H-MR spectroscopy: a single voxel study of the cerebellar vermis in patients with degenerative ataxias. *J Magn Reson Imaging*. 2009; 30(1):11–17. [PubMed: 19557841]
58. Currie S, Hadjivassiliou M, Wilkinson ID, Griffiths PD, Hoggard N. Magnetic Resonance Spectroscopy of the Normal Cerebellum: What Degree of Variability Can Be Expected? *Cerebellum*. 2013; 12(2):205–211. [PubMed: 22987337]
59. Mascalchi M, Brugnoli R, Guerrini L, Belli G, Nistri M, Politi LS, Gavazzi C, Lolli F, Argenti G, Villari N. Single-voxel long TE 1H-MR spectroscopy of the normal brainstem and cerebellum. *Journal of Magnetic Resonance Imaging*. 2002; 16(5):532–537. [PubMed: 12412029]
60. Delamillieure P, Constans JM, Fernandez J, Brazo P, Benali K, Courtheoux P, Thibaut F, Petit M, Dollfus S. Proton magnetic resonance spectroscopy (1H MRS) in schizophrenia: investigation of

the right and left hippocampus, thalamus, and prefrontal cortex. *Schizophr Bull.* 2002; 28(2):329–339. [PubMed: 12693438]

61. Nage-Poetscher LM, Bonekamp D, Barker PB, Brant LJ, Kaufmann WE, Horska A. Asymmetry and gender effect in functionally lateralized cortical regions: a proton MRS imaging study. *J Magn Reson Imaging.* 2004; 19(1):27–33. [PubMed: 14696217]
62. Golden CJ, Graber B, Coffman J, Berg RA, Newlin DB, Bloch S. Structural brain deficits in schizophrenia. Identification by computed tomographic scan density measurements. *Arch Gen Psychiatry.* 1981; 38(9):1014–1017. [PubMed: 7283660]
63. Cullen TJ, Walker MA, Eastwood SL, Esiri MM, Harrison PJ, Crow TJ. Anomalies of asymmetry of pyramidal cell density and structure in dorsolateral prefrontal cortex in schizophrenia. *Br J Psychiatry.* 2006; 188:26–31. [PubMed: 16388066]
64. Henry PG, Dautry C, Hantraye P, Bloch G. Brain GABA editing without macromolecule contamination. *Magn Reson Med.* 2001; 45(3):517–520. [PubMed: 11241712]
65. Edden RA, Puts NA, Barker PB. Macromolecule-suppressed GABA-edited magnetic resonance spectroscopy at 3T. *Magn Reson Med.* 2012; 68(3):657–661. [PubMed: 22777748]
66. Dydak U, Jiang YM, Long LL, Zhu H, Chen J, Li WM, Edden RA, Hu S, Fu X, Long Z, Mo XA, Meier D, Harezlak J, Aschner M, Murdoch JB, Zheng W. In vivo measurement of brain GABA concentrations by magnetic resonance spectroscopy in smelters occupationally exposed to manganese. *Environ Health Perspect.* 2011; 119(2):219–224. [PubMed: 20876035]

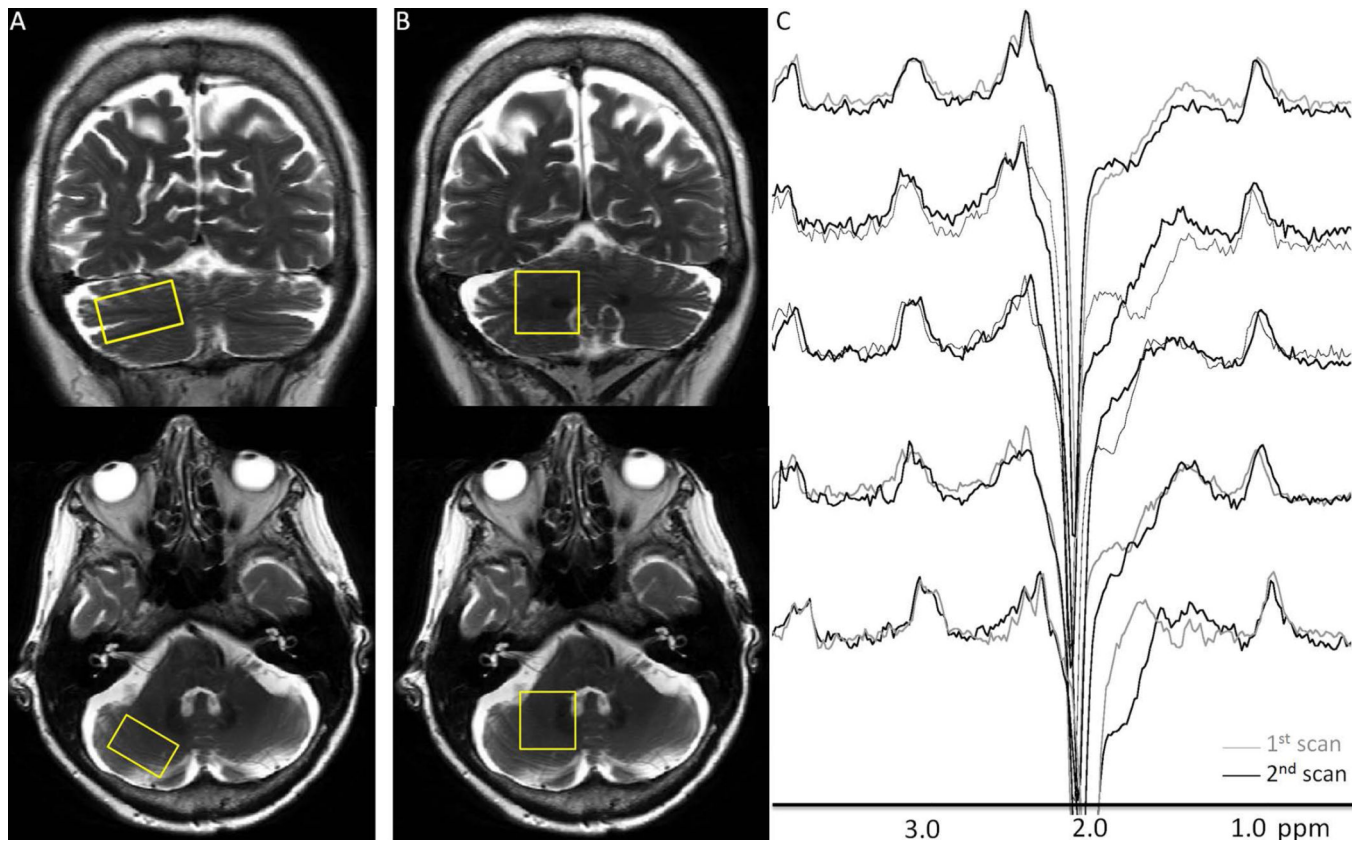


Figure 1. Representative right cerebellar cortex (A) and dentate (B) voxel placements on T2-weighted coronal and axial slices. Short TE data were obtained from both VOIs, whereas GABA spectra were only obtained from the dentate VOIs. (C) shows pairs of repeated right cerebellar dentate GABA-edited difference spectra. Good visual correspondence was observed between the repeated measurements.

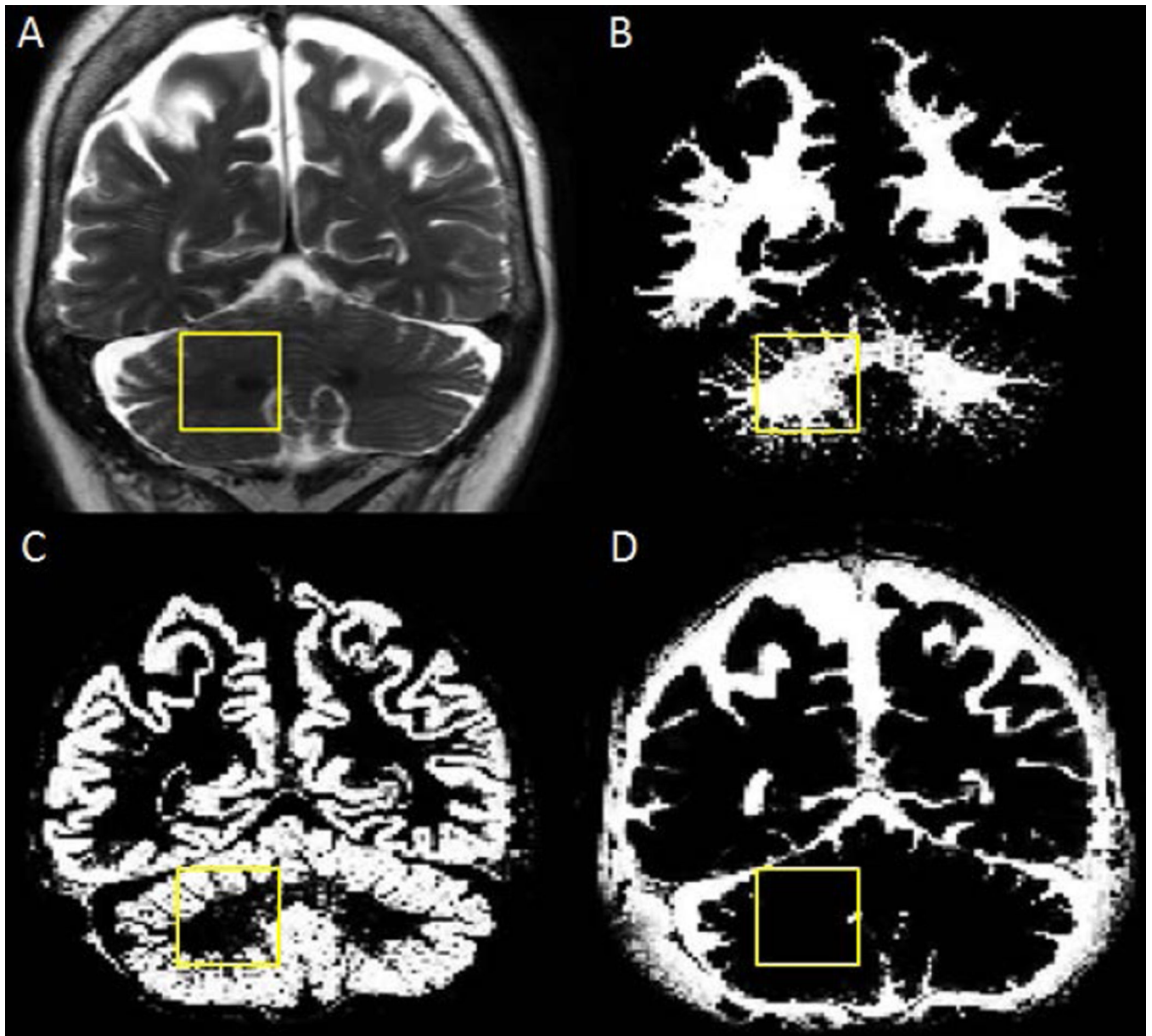


Figure 2. Representative tissue segmentation of the cerebellum: (A) T2-weighted image showing the right cerebellar dentate VOI from Figure 1. (B), (C) and (D) show white matter, gray matter and cerebrospinal fluid maps of the same slice, respectively.

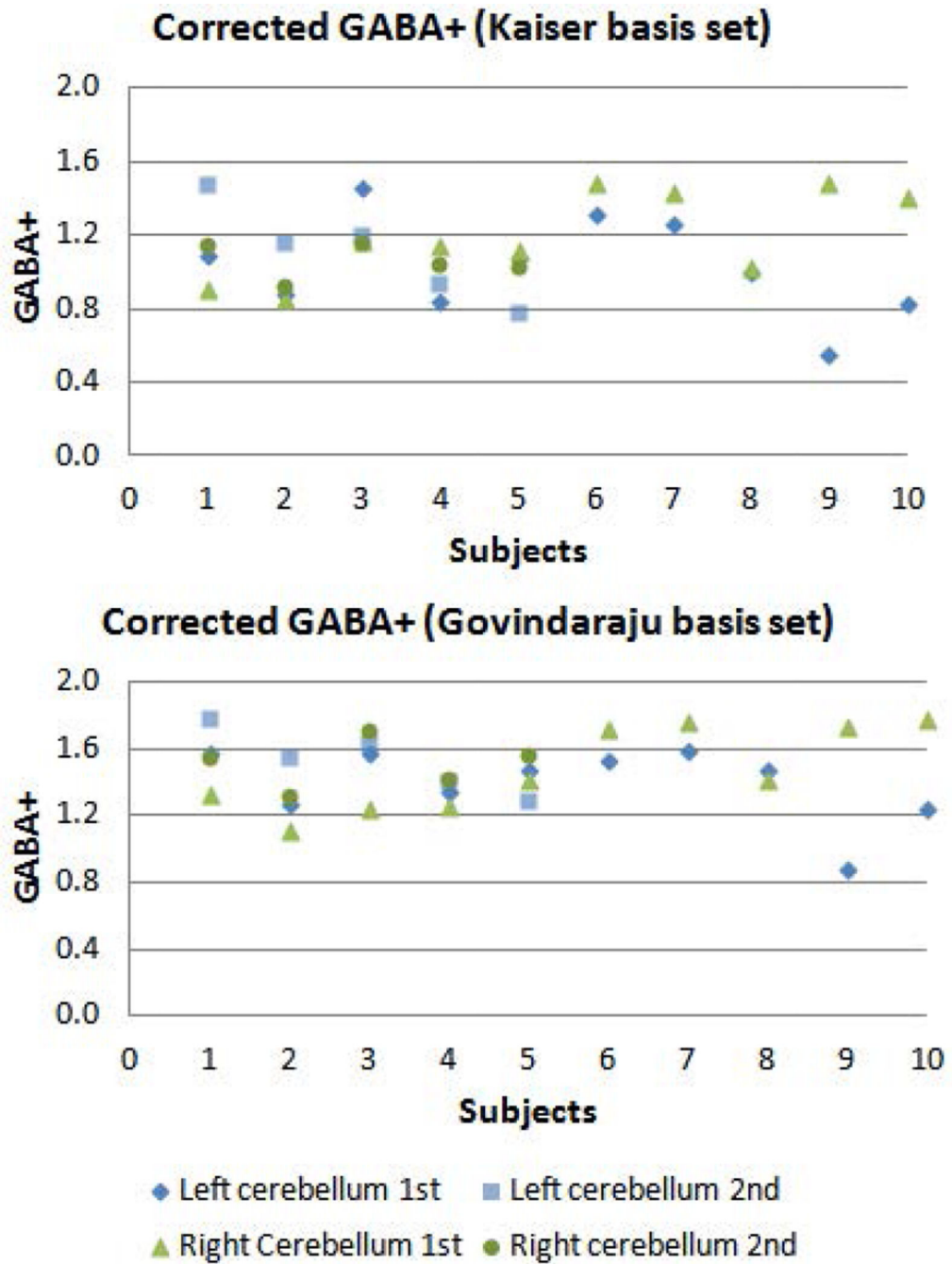


Figure 3. GABA+ levels corrected for tissue composition and relaxation effects in left and right cerebellar dentate VOIs from all subjects. 5 subjects underwent 1st and 2nd scans in order to assess short-term reproducibility.

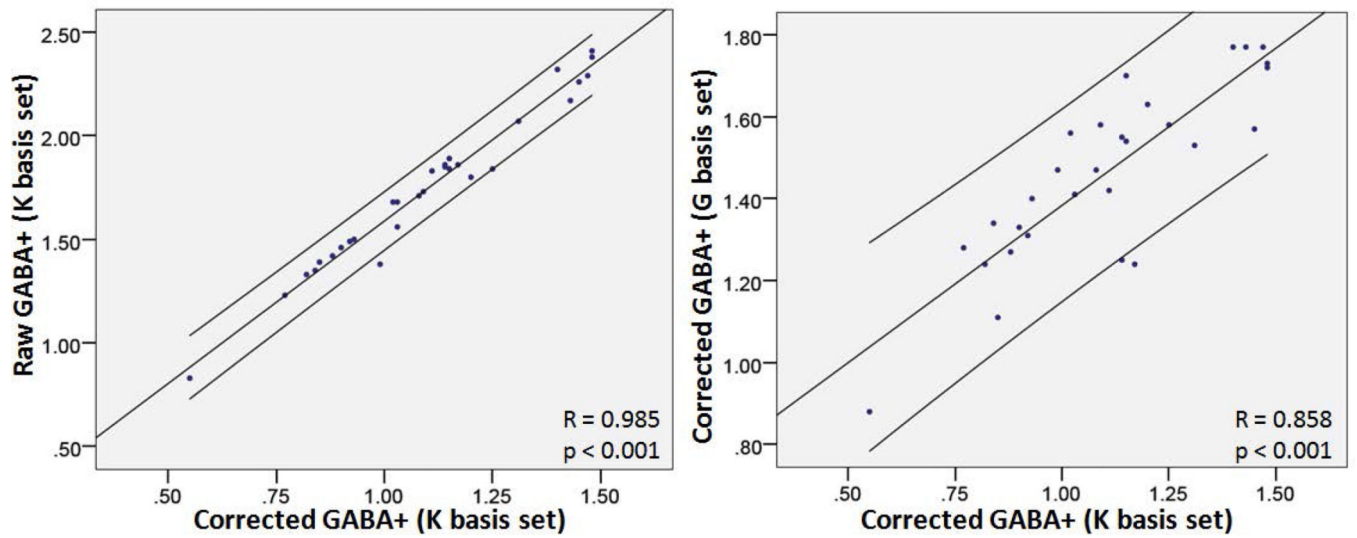


Figure 4. Scatter plots of correlation between corrected GABA+ and raw GABA+ using the Kaiser basis set (Left) and corrected GABA+ between using Kaiser and Govindaraju basis sets (Right), obtained from LCMoel analysis, with a 95 % confidence interval.

Chemical shifts and J-coupling constants from two previous publications used for generating GABA ($\text{NH}_2\text{-}^4\text{CH}_2\text{-}^3\text{CH}_2\text{-}^2\text{CH}_2\text{-}^1\text{COOH}$) basis sets.

Table 1

	Chemical Shift (ppm)		J-coupling (Hz)								
	$^2\text{CH}_2$	$^3\text{CH}_2$	$^4\text{CH}_2$	J_{2-3}	$\text{J}_{2,3'}$	$\text{J}_{2',3}$	$\text{J}_{2'-3'}$	J_{3-4}	$\text{J}_{3,4'}$	$\text{J}_{3',4}$	$\text{J}_{3'-4'}$
Govindaraju et al.(45)	3.0128	1.8890	2.2840	5.372	7.127	10.578	6.982	7.755	7.432	6.173	7.933
Kaiser et al.(46)	2.284	1.888	3.012	7.352	7.352	7.352	7.352	6.377	7.960	8.139	7.495

Table 2

Raw and corrected mean GABA+ levels in institutional units obtained from GABA-edited spectra using LCMModel with two basis sets (abbreviated as K basis set and G basis set), and corresponding intra-individual and inter-individual coefficients of variation (CVs).

	Left Cerebellar Dentate						Right Cerebellar Dentate					
	K basis set			G basis set			K basis set			G basis set		
	Levels	Intra-individual CVs (%)	Inter-individual CVs (%)	Levels	Intra-individual CVs (%)	Inter-individual CVs (%)	Levels	Intra-individual CVs (%)	Inter-individual CVs (%)	Levels	Intra-individual CVs (%)	Inter-individual CVs (%)
Raw GABA+	1.64 ± 0.39	12.0 ± 3.7	23.6	2.24 ± 0.32	4.7 ± 3.1	14.2	1.86 ± 0.32	5.0 ± 3.7	17.3	2.40 ± 0.34	8.7 ± 4.3	14.1
Corrected GABA+	1.05 ± 0.25	11.9 ± 4.1	23.9	1.44 ± 0.21	5.3 ± 2.9	14.4	1.15 ± 0.20	5.0 ± 3.7	17.6	1.49 ± 0.21	8.5 ± 3.7	14.1
Raw GABA+/Cr	0.17 ± 0.04	13.9 ± 6.9	25.6	0.23 ± 0.03	6.6 ± 5.0	14.5	0.19 ± 0.05	6.9 ± 7.0	27.0	0.25 ± 0.05	9.5 ± 2.5	21.3
Corrected GABA+/Cr	0.22 ± 0.05	13.4 ± 6.3	24.2	0.30 ± 0.04	6.1 ± 4.8	13.7	0.25 ± 0.05	5.0 ± 2.9	20.9	0.32 ± 0.05	8.0 ± 3.6	16.4
Raw GABA+/NAA	0.15 ± 0.03	9.4 ± 7.3	20.4	0.21 ± 0.03	5.1 ± 3.5	13.2	0.17 ± 0.02	7.9 ± 5.1	14.8	0.22 ± 0.03	9.8 ± 8.6	14.1
Corrected GABA+/NAA	0.24 ± 0.05	11.5 ± 4.2	22.1	0.33 ± 0.04	4.4 ± 2.8	12.6	0.27 ± 0.05	4.0 ± 2.8	18.1	0.35 ± 0.05	9.3 ± 5.9	15.6

Table 3

Raw and corrected mean metabolite levels in institutional units obtained from short-TE spectra using LCModel from all subjects, and corresponding intra-individual and inter-individual coefficients of variation (CVs).

	Left Cerebellar Dentate			Right Cerebellar Dentate			Left Cerebellar Cortex			Right Cerebellar Cortex		
	Levels	Intra-individual CVs (%)	Inter-individual CVs (%)	Levels	Intra-individual CVs (%)	Inter-individual CVs (%)	Levels	Intra-individual CVs (%)	Inter-individual CVs (%)	Levels	Intra-individual CVs (%)	Inter-individual CVs (%)
Raw Cr	7.00 ± 0.77	2.8 ± 2.1	10.9	6.95 ± 0.62	3.4 ± 2.3	9.0	8.09 ± 0.68	2.9 ± 1.6	8.3	7.62 ± 0.58	1.2 ± 0.8	7.6
Corrected Cr	4.87 ± 0.61	3.0 ± 1.7	12.6	4.65 ± 0.50	3.2 ± 2.0	10.7	5.57 ± 0.76	4.6 ± 1.9	9.9	5.16 ± 0.57	4.4 ± 4.4	11.1
Raw NAA	6.79 ± 0.32	1.3 ± 0.6	4.7	6.97 ± 0.47	3.4 ± 2.0	6.7	6.83 ± 0.42	2.6 ± 1.4	6.1	5.40 ± 0.26	1.2 ± 0.6	4.8
Corrected NAA	4.35 ± 0.17	1.3 ± 0.5	4.0	4.31 ± 0.33	3.7 ± 2.0	7.6	4.34 ± 0.36*	3.0 ± 1.5	8.2	3.37 ± 0.25*	4.3 ± 3.2	7.3
Corrected NAA/Cr	0.91 ± 0.11	2.1 ± 2.5	12.1	0.93 ± 0.09	5.4 ± 3.0	10.1	0.78 ± 0.07	3.0 ± 1.4	8.4	0.66 ± 0.06	1.5 ± 1.0	8.4
Raw Glu	5.53 ± 0.79	3.7 ± 2.9	14.3	5.99 ± 0.93	5.8 ± 2.9	15.5	6.60 ± 0.69	5.5 ± 4.6	10.5	5.67 ± 0.50	4.4 ± 0.7	8.9
Corrected Glu	3.73 ± 0.50	3.4 ± 2.4	13.5	3.89 ± 0.60	5.4 ± 3.0	15.4	4.40 ± 0.43	4.6 ± 4.4	9.8	3.72 ± 0.41	5.5 ± 0.5	11.1

* p<0.01 when comparing left versus right cerebellar cortex.

Table 4

Relative voxel tissue composition in 4 volumes of interest--left and right cerebellar dentate and cortex, from all subjects (Mean \pm SD (range)).

	Left Cerebellar Dentate	Right Cerebellar Dentate	Left Cerebellar Cortex	Right Cerebellar Cortex
GM	54.3 \pm 3.5 (47.8 ~ 61.0)	52.0 \pm 3.7 (45.8 ~ 58.9)	62.6 \pm 6.3 (50.9 ~ 70.8)	59.5 \pm 6.9 (50.9 ~ 72.4)
WM	40.5 \pm 3.7 (31.7 ~ 45.2)	45.0 \pm 4.1 (35.1 ~ 49.3)	33.9 \pm 7.3 (23.2 ~ 47.9)	37.8 \pm 9.0 (15.2 ~ 47.4)
CSF	5.2 \pm 2.6 (2.3 ~ 11.9)	3.0 \pm 1.5 (1.4 ~ 6.0)	3.5 \pm 2.6 (0.8 ~ 8.7)	2.7 \pm 3.0 (0.3 ~ 12.4)